Large-Signal, Dynamic, Negative Conductance of Gunn Devices in Sharpless Flanges

MYSORE R. LAKSHMINARAYANA, MEMBER, IEEE, AND LARRY D. PARTAIN, MEMBER, IEEE

Abstract—**A good agreement between actual, large-signal Gunn device operation and a first principles model has been achieved in terms of descriptive device parameters. An injection-locking technique was used to measure the variations of device conductance and capacitance with RF voltage amplitude. The equivalent circuits developed allow optimization of Gunn oscillator circuits.**

I. Introduction

THE LARGE-SIGNAL ac conductance and susceptance of Gunn devices determines their behavior in microwave circuit applications. The large-signal ac conductance of Gunn device oscillators is specified as bing equal to the negative of the stabilizing conductance [1], [2] introduced into the circuit. Recently, techniques have been developed to measure large-signal properties of oscillating Gunn devices by a transient method [3] and by an injection-locking method [4]. However, these experimental results have not been successfully modeled theoretically. In this paper, the injection-locking technique has been used to measure the large-signal ac conductances and susceptances of oscillating Gunn devices mounted in Sharpless [5]–[7] flanges and coaxial circuits. This data has been compared to a first principles device theory developed in an earlier paper [8]. This study represents the first lumped element, equivalent circuit modeling of a Gunn device in a Sharpless flange. The Sharpless flange mount provides bias filtering, efficient heat sinking, iris coupling, rugged construction, and minimum intrusion into resonant cavities.

In the theoretical treatments of Section II, the predicted values of large-signal ac conductance and susceptance are given, the lumped element, equivalent circuit for the Sharpless flange is developed, and the equivalent impedance of a cavity resonator is given. The predicted impedance of the flange alone is presented and all the elements are combined into a system equivalent circuit that models the frequency tuning characteristics of the oscillator. In Section III, the method for measuring the large-signal ac impedance by injection locking is described. In the results of Section IV, the measured conductance and susceptance of the Gunn device itself are compared to the predicted values. The measured tuning curve for the Sharpless flange circuit is compared to the theoretical curve, and the experimentally measured impedance of the Sharpless flange is compared to the theoretical curve.

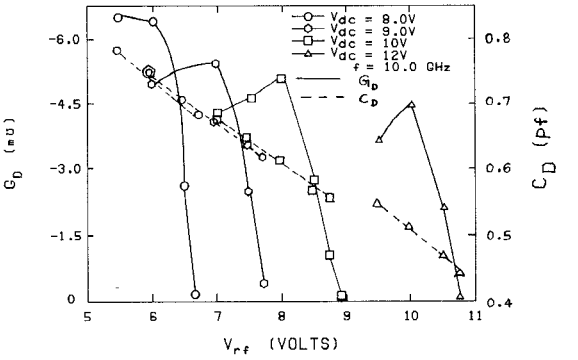

Fig. 1. The theoretical Gunn device values of negative conductance and capacitance as a function of RF voltage amplitude for various dc-bias voltages at 10 GHz.

II. Device Oscillator Theory

The theoretical values of Gunn device conductance G_D and capacitance C_D obtained with numerical simulation developed in an earlier paper [8] for a Microwave Associates MA49158 Gunn device are shown in Fig. 1 as a function of the RF voltage amplitude for various dc-bias voltages. Note that the magnitude of G_D passes through a maximum. In regions of positive slope, a small perturbation increasing V_{RF} would also increase the conductance magnitude leading to a further increase in V_{RF} and instability. Thus, the only stable regions of operation are for V_{RF} values past the maximum where the slope is negative.

The GaAs chip for a MA49158 device mounted in a $S4$ package has been well modeled by Getsinger [9], [10] and by Owens and Cawsey [11] in terms of capacitance C_1 and C_2 and an inductor L_1 as shown in Fig. 2 between terminals T^*–T and T_D^*–T_D. These components have the values $C_1 = 0.05$ pF, $C_2 = 0.21$ pF, and $L_1 = 0.64$ nH. This packaged device was included in a Sharpless flange [5]–[7] with the dimensions shown in Fig. 3. The insulated dc-bias terminal rod provides a convenient method of furnishing dc power to the device. The capacitance between the rod and the grounded metal body of the flange and the induc-

Manuscript received May 3, 1982; revised September 9, 1982. This study was performed by the authors in the Electrical Engineering Department, University of Delaware, Newark, DE 19711.

M. R. Lakshminarayana is now with the Electrical Engineering Department, California State Polytechnic University, Pomona, CA 91768

L. D. Partain is now with the Chevron Research Company, Richmond, CA 94802

0018-9480/83/0300-0265$01.00 ©1983 IEEE

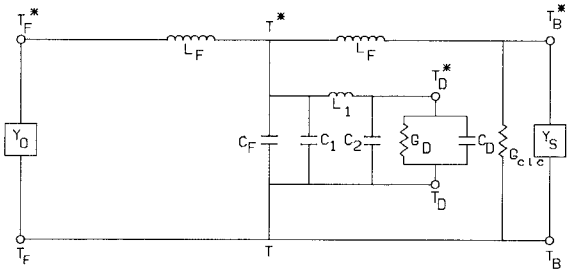

Fig. 2. The lumped element, equivalent circuit for the total system composed of the Gunn device, its package, the Sharpless flange, the resonant cavity, and the waveguide load.

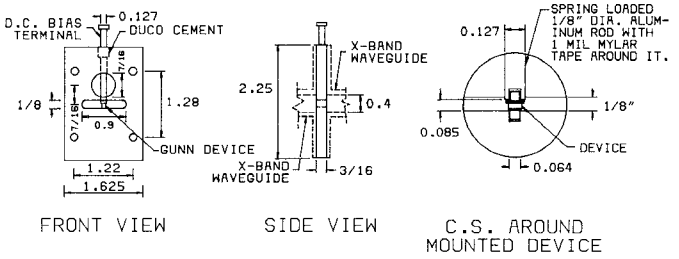

Fig. 3. The Sharpless flange mounting for the package Gunn device. All dimensions are given in inches.

tance encountered with the 7/16-in-diameter hole provide a low-pass filter that prevents RF frequencies generated at the device from reaching the dc-bias terminal. The mounting of the Gunn device in the 1/8-in-wide iris slot allows efficient heat sinking. The 400°K temperature used for the preceding theoretical calculations is typical of Gunn devices operated in this manner with an adequate heat sink [12]. According to Heaton and Ramachandran [12], the heat sink is sufficient if the threshold current of the mounted device is greater than 0.95 of the factory tested value. This criterion was met for the mounted devices measured in this investigation.

The lumped element equivalent circuit description of the composite microwave structure shown in Fig. 3 in the form of a capacitive iris has been developed from Marcuvitz's treatment [13] in terms of two inductances L_F and a capacitance C_F as shown in Fig. 2 where the terminals $T_F^*-T_F$ and $T_B^*-T_B$ represent the planes at each side of the flange as presented to connecting X-band rectangular waveguides (see Fig. 3, side view), and where the terminal T^*-T is the plane cutting the flange in half at the center of the iris. The theoretical values shown by the solid line curve in Fig. 4 are the magnitude of input impedance that this equivalent circuit gives as a function of frequency locking in the $T_F^*-T_F$ plane with a matched load connected to terminals $T_B^*-T_B$ and no device or package mounted in the flange iris. This is used later to establish the validity of the equivalent circuit for the flange.

If a cavity is formed by connecting the Sharpless flange to a tuning short of length l at the plane $T_B^*-T_B$, the admittance of this short Y_S is a susceptance B_S so that

$$Y_S = jB_S = -jY_o \cot \frac{2\Pi l}{\lambda g} \tag{1}$$

where λ_g is the guided wavelength. Accounting for the

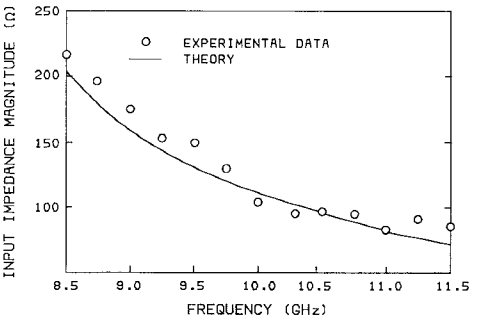

Fig. 4. The theoretical and measured values of input impedance as a function of frequency of the empty (no Gunn Device or device package) Sharpless flange terminated on one side by an X-band waveguide connected to a matched load.

losses due to cavity walls and device mount by the loss conductance G_{CLC} then gives the composite equivalent circuit of Fig. 2 for the Gunn flange oscillator with the output (at plane $T_F^*-T_F$) connected to a matched waveguide load of characteristic admittance Y_o. A means for determining values for all the elements in this circuit have been given with the exception of G_{CLC}. Although G_{CLC} can be estimated from the wall losses or cavity Q measurements, exact value G_{CLC} is difficult to determine. Accurate value of G_{CLC} may be measured by using a miniature coaxial probe across the T^*-T terminals (looking towards the short) with the packaged device disconnected from those terminals. Authors did not pursue this measurement technique. If this equivalent circuit, except for G_D and C_D, is reduced to an equivalent load conductance G_{DL} and equivalent load susceptance B_{DL} that loads the device chip at the terminals $T_D^*-T_D$, then the stable oscillation condition of no net power loss and zero-phase shift requires that

$$G_T = G_{DL} + G_D = 0 \tag{2}$$

and

$$B_T = B_{DL} + 2\Pi f C_D = 0. \tag{3}$$

As stated earlier, stable amplitude performance requires that $-dG_D/dV_{\mathrm{RF}} < 0$. When combined with an oscillator system, the changes in G_{DL} with V_{RF} must be of the same sign or be small enough with the opposite sign to allow

$$\frac{d}{dV_{\mathrm{RF}}}(G_{DL} + G_D) = \frac{dG_T}{dV_{\mathrm{RF}}} > 0 \tag{4}$$

if stable output power is to be achieved. Similar frequency stability arguments related to phase shift and discussed by Kurokawa [14], [15] require that

$$\frac{dB_T}{df} > 0. \tag{5}$$

These considerations allow the frequency tuning characteristics of the total Gunn flange oscillator to be modeled. The numerical simulation program [8] was used to calculate values of C_D as a function of the frequency with dc-bias voltage of 10 V and an amplitude of V_{RF} of 8 V. The distance l the short would need to be from the flange, to satisfy the zero-phase condition of (3), was then calculated. The results of this are plotted as the solid line curve in Fig. 5. For reference, the frequency specified by $l = \lambda_g/2$

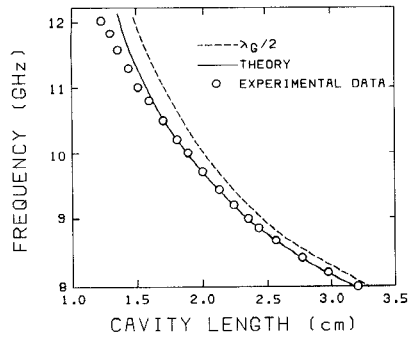

Fig. 5. The experimental and theoretical values of frequency of the Sharpless flange oscillator system as a function of the length between the flange and the waveguide short.

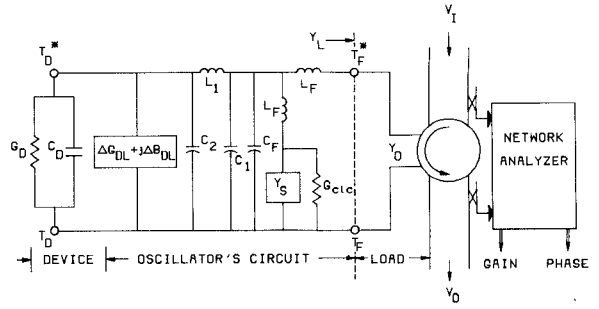

Fig. 6. The circuit configuration for the injection-locked measurements of the Sharpless flange, Gunn oscillator system.

is shown as the dashed line, spaced a small distance away. Comparison shows that the oscillator susceptance is dominated by the position of the short but that the frequency is significantly shifted by the device and flange reactances.

III. Device Measurement Theory

The zero-loss and phase-shift conditions of (2) and (3) require that when stable operation is achieved, one can be sure that device conductance is given by

$$G_D = -G_{DL} \quad \text{and} \quad C_D = -\frac{B_{DL}}{2\Pi f}. \tag{6}$$

Thus, if the load impedance

$$Y_{DL} = G_{DL} + jB_{DL} \tag{7}$$

can be varied in known ways, the device values of G_D and C_D can be determined as a function of these variations. From the theoretical plots of Fig. 1, where stable operation is for V_{RF} values past the points of maximum magnitude in G_D, one would expect that V_{RF} will increase as G_{DL} decreases so that (2) remains satisfied. The output power at the terminals $T_F^* - T_F$ should reflect such variations in V_{RF} at the device.

A convenient way of providing controlled changes in the load presented to an oscillator while monitoring its output power can be achieved by injection locking. Injection locking is the phenomenon observed with free-running oscillators, where injecting an external signal into the oscillator circuit at a frequency not too far from its free-running value causes the oscillator to change its frequency to the injected signal frequency but at a constant phase difference between the injected and output signals. This follows from Adler's original small-signal work on vacuum tube oscillators [16] which was later extended to large signals by Paciorek [17]. Recently Young and Stephenson [4] have used injection locking to characterize Gunn and IMPATT devices in coaxial cavity oscillator circuits. This approach was utilized for this study as illustrated by the system shown in Fig. 6. A circulator was used to inject an RF signal (represented by a phasor with complex value V_I) into the output terminals $T_F^* - T_F$ of the Gunn flange oscillator and to monitor the output signal of complex voltage value V_o. The ratio of the amplitudes of V_o and V_I and the phase angle between them were conveniently determined with a network analyzer connected to the input and output signals through directional couplers.

Looking from the oscillator toward the circulator at the terminals $T_F^* - T_F$, the incident signal is V_o and the reflected signal is V_I so that the reflection coefficient Γ is

$$\Gamma = \frac{V(\text{reflected})}{V(\text{incident})} = \frac{V_I}{V_o} = \rho e^{-j\phi} \tag{8}$$

where ρ is the magnitude $|V_I/V_o|$ and ϕ is the phase angle between V_I and V_o at the plane $T_F^* - T_F$. This reflection coefficient defines the equivalent load impedance Y_L presented to the oscillator at the terminals $T_F^* - T_F$ as

$$Y_L = G_L + jB_L = Y_o\left[\frac{1-\rho^2}{1+\rho^2+2\rho\cos\phi}\right] + jY_o\left[\frac{2\rho\sin\phi}{1+\rho^2+2\rho\cos\phi}\right] \tag{9}$$

which shows that Y_L changes as the ratio $|V_I/V_o| = \rho$ is varied by injecting stronger or weaker signals. With $V_I = 0$, Y_L just equals Y_o. For very large V_I's, V_o is essentially the injected signal V_I phase shifted so that ρ approaches one, and the rest part of Y_L is arbitrarily small. As ρ varies, ϕ also varies in a highly symmetric manner dependent on the frequency difference between the injected signal and the free-running oscillator frequency. This was described theoretically by Michaelides and Stephenson [18].

Standard circuit analysis of the equivalent circuit of Fig. 6 allows any value of Y_L at $T_F^* - T_F$ to be used to determine what new admittance values are presented to the device at $T_D^* - T_D$ for each new value of Y_L. Thus, a variable load Y_{DL} is obtained as a function of Y_L to give $Y_{DL}(Y_L)$. For convenience, the case when $G_{CLC} = 0$ can be used to define $Y_{DL}^\circ = G_{DL}^\circ + jB_{DL}^\circ$ as

$$Y_{DL}(Y_L)|_{G_{CLC}=0} = Y_{DL}^\circ(Y_L). \tag{10}$$

Since, in general, this differs from the $G_{CLC} \neq 0$ values, correction terms ΔG_{DL} and ΔB_{DL} can be defined by

$$G_{DL}(Y_L) = G_{DL}^\circ(Y_L) + \Delta G_{DL}(Y_L) \tag{11}$$

$$B_{DL}(Y_L) = B_{DL}^\circ(Y_L) + \Delta B_{DL}(Y_L). \tag{12}$$

Since accurate values of G_{CLC} are unavailable, the zero-loss $G_{DL}^\circ(Y_L)$ and $B_{DL}^\circ(Y_L)$ values are the most easily determined. The desired values of the device conductance

and capacitance are given in terms of these as

$$G_D = -G^{\circ}_{DL}(Y_L) - \Delta G_{DL}(Y_L) \tag{13}$$

and

$$C_D = -\frac{B^{\circ}_{DL}(Y_L) + \Delta B_{DL}(Y_L)}{2\Pi f}. \tag{14}$$

The above indicates the experimental technique used for measuring G_D and C_D values to within the uncertainty factors ΔG_{DL} and ΔB_{DL}. To compare with the theory of Fig. 1, V_{RF} also needs to be found simultaneously. The power output of the oscillator P_{OSC} must equal the power developed in the load impedance $Y_L = G_L + jB_L$ at the terminals $T_F^* - T_F$ specified by

$$P_{\mathrm{OSC}} = \frac{G_L}{2}|V_{TF}|^2 \tag{15}$$

where G_L is determined by (9) and V_{TF} is the sum of the phasers V_I plus V_o at $T_F^* - T_F$. The magnitude of V_{TF} is given by

$$\begin{aligned}|V_{TF}| &= \left[|V_o|^2 + |V_I|^2 + 2|V_o||V_I|\cos\phi\right]^{1/2} \\ &= \left[\frac{2P_o}{Y_o}\right]^{1/2}\left[1 + \rho^2 + 2\rho\cos\phi\right]^{1/2}\end{aligned} \tag{16}$$

where P_o is the output power of the injection-locked oscillator determined by V_o. From conservation of energy, this oscillator supplied power must equal the power developed in the negative conductance of the Gunn device minus that lost in the cavity due to G_{CLC} so that

$$P_{\mathrm{OSC}} = \frac{V_{\mathrm{RF}}^2}{2}|G_D| - \frac{V_{\mathrm{RF}}^2}{2}\Delta G_{DL}(Y_L) \tag{17}$$

which reduces to

$$\begin{aligned}P_{\mathrm{OSC}} &= \frac{V_{\mathrm{RF}}^2}{2}\left[G^{\circ}_{DL}(Y_L) + \Delta G_{DL}(Y_L)\right] - \frac{V_{\mathrm{RF}}^2}{2}\Delta G_{DL}(Y_L) \\ &= \frac{V_{\mathrm{RF}}^2}{2}G^{\circ}_{DL}(Y_L).\end{aligned} \tag{18}$$

From (14)–(17)

$$V_{\mathrm{RF}} = \left[\frac{G_L}{G^{\circ}_{DL}(Y_L)}\right]^{1/2}\left[\frac{2P_o}{Y_o}\right]^{1/2}\left[1 + \rho^2 + 2\rho\cos\phi\right]^{1/2} \tag{19}$$

where ρ, ϕ, and P_o are measured and $G^{\circ}_{DL}(Y_L)$ is calculated from the Fig. 6 equivalent circuit (with $G_{CLC} = 0$) using the measured value of $Y_L = G_L + jB_L$ specified by (9).

The major disadvantage of the Sharpless flange oscillator measurement described above is its inability to adjust for the influence of the unknown loss conductance G_{CLC}. This disadvantage can be overcome if measurements can be made of the cavity resonator admittance Y_{DL} directly at the terminals of the device package ($T^* - T$ of Fig. 2). With the device mounted in a coaxial resonator and free running (no injected signal), the circuit can be disconnected from the device and connected directly to coaxial connectors of a network analyzer for a direct measurement of the free-running Y_{DL}. This permits the determination of Y_{DL} as a function of V_{RF} by the transformer method described in Appendix A.

IV. Results

Measurements were performed at a frequency of 10 GHz on a Microwave Associates MA49158 Gunn device mounted in an *S*4 package. Sharpless flange data was obtained for the device inserted into the flange of Fig. 3. It was connected on both sides to rectangular waveguide. One side of this waveguide was shorted at a distance 0.74 in from the flange to form a 10-GHz resonant structure. The other side was connected to a circulator and the Hewlett-Packard Model 8410B network analyzer as shown in Fig. 6.

The coaxial cavity results were obtained with the Gunn device mounted between the center conductor and a conducting disk attached to the outer cylindrical conductor at one end of the cavity. The other end was terminated by a variable short adjusted to a distance of approximately 0.59 in from the device to provide oscillations at 10 GHz. The dc power was inserted through a coaxial bias *T* which provided a low-pass filter to prevent high frequencies from reaching the dc power supply. Output power and signal injection were obtained by radially inserting a capacitive probe into the side of the cavity using a 50-Ω coaxial cable.

Because the network analyzer ports are at some constant distance from the plane $T_F^* - T_F$ of Fig. 6 (and Fig. 9, see Appendix A), the measured phase angle θ differed from the load impedance Y_L, *s* phase angle ϕ by a constant amount ψ so that $\phi = \theta - \psi$. Data obtained by injection locking the Gunn flange oscillator are shown in Fig. 7 for the free-running oscillation frequency of 10 GHz and a dc-bias voltage of 10 V. The results are plotted as the measured phase angle versus the gain defined as P_o/P_I where P_I is the power level of the injected signal. The injected power level and frequency were varied as the experimental control parameters to obtain the data. Different curves were obtained depending on how much the injected signal frequency f_I differed from the free-running frequency f (i.e., $\Delta f = f_I - f$). According to the theoretical treatment of Young and Stephenson, [4], these curves should be symmetrically distributed about $\phi = 0$. This allowed the constant phase difference of $\psi = 281$ degrees to be identified. This data is the first clear experimental verification of the theoretically predicted, symmetrical form for the phase-gain relations for Gunn oscillators. Earlier measurements contained such large errors that the symmetry was not clearly demonstrated [4].

The values of the device negative conductance (assuming zero-cavity loss, $G_{CLC} = 0$ and $\Delta G_{DL} = 0$) were obtained from the values of Y_L measured with the network analyzer as the injected signal strength P_I was varied for a Δf value of zero. The equivalent circuit of Fig. 6 was used to calculate $G^{\circ}_{DL}(Y_L)$ as a function of V_{RF} (which was calculated from measured P_o values using (19)). Multiplying these conductance values by minus one gives the "zero-cavity loss" values shown by the square data point in Fig. 8.

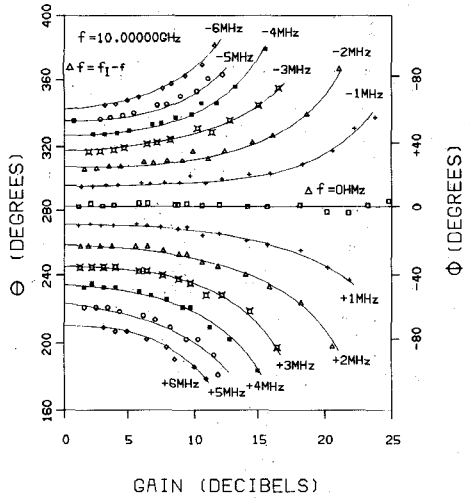

Fig. 7. The measured phase-gain characteristics of the Sharpless-flange Gunn-oscillator system obtained by injection locking.

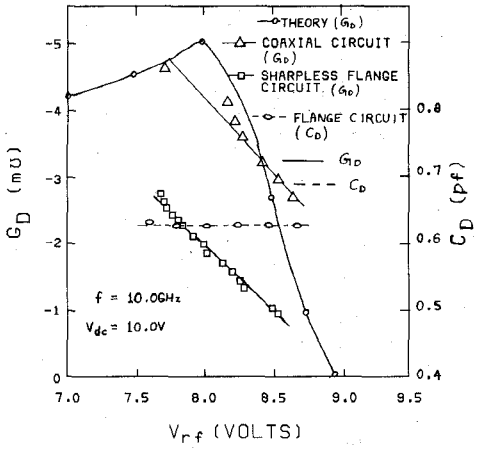

Fig. 8. The negative conductance of the Gunn device as a function of RF voltage obtained for the Sharpless-flange arrangement of Fig. 6 and the coaxial circuit of Fig. 9.

These differ from the device negative conductance by the unknown cavity loss term $\Delta G_{DL}(Y_L)$ described in (11).

For comparison the device negative conductance obtained with the coaxial cavity and the transformer equivalent circuit analysis is shown by the triangular data points in Fig. 8 for a dc-bias voltage of 10 V and an oscillation frequency of 10 GHz. For comparison, the theoretically predicted values given in Fig. 1 are plotted in Fig. 8 as the circular data points and the solid line curve. Note that the absolute values of the experimental and theoretical curves agree to within 30 percent, the RF voltages for maximum G_D agree to within 7 percent for coaxial circuit measurement and agree to within 50 percent for the flange circuit measurement and the negative slope of G_D versus V_{RF} agree to within a factor of two. The device capacitance C_D obtained from the injection-locked Sharpless flange data is also shown in Fig. 8. It agrees with the theoretical values of Fig. 1 to within 20 percent although the theory shows a downward slope with V_{RF} not evident in the measured data. This difference is probably due to the theoretical model which only used the fundamental component of current waveform for the reactance calculations. The large loss (approximately 50 percent) is a significant disadvantage of the specific Sharpless flange configuration used in this study.

The tuning curves for the Sharpless flange oscillator were obtained by replacing the shorted section of X-band waveguide with a tuneable short. Frequency variation was achieved by moving the position of the short relative to the flange. The results are shown by the circular data points in Fig. 5. It agrees with the theory to within 3 percent between 8 and 10.5 GHz and to within 14 percent between 10.5 and 12 GHz.

As a check of the equivalent circuit used to model the flange itself, the Gunn Device was removed from the Sharpless flange and the flange alone was connected to the network analyzer where its transmission and reflection coefficients were determined as a function of frequency. This was converted into input impedance by standard equations and plotted as the circular data points in Fig. 4. The agreement with theory is within 13 percent which serves as a verification of the equivalent circuit for the flange developed here for the first time from Marcuvitz's theory [13].

V. Conclusions

Injection locked measurements of the large-signal conductance and susceptance of Gunn devices has provided data that agrees well with the theoretically predicted values of device conductance, its variation with RF voltages, and with theoretical values of device capacitance and with the predicted tuning curves. Ideal matching of a device to its resonant circuit and its load requires that the flange provide appropriate coupling. Calculations with the flange circuit should allow such coupling to be achieved for any negative resistance device of known characteristics. The agreement between theoretical and experimental values of the flange impedance and for the device tuning curve demonstrates the accuracy of the equivalent circuit. Its use should allow analysis and optimization of Gunn device oscillators and systems. The increased errors associated with C_D due to harmonic energy storage currents is evident from the measured and modeled values. Good agreement was found for absolute values of C_D, but there was a difference in the theoretical and measured variations with signal amplitude.

Appendix A
Transformer Equivalent Circuit Analysis

Directly connecting a coaxial resonant circuit to a network analyzer at the point where a device can be inserted allows the impedance presented to the device to be directly measured. However, injection locking is not possible since the device is no longer present to be injection locked. When the device is returned to the coaxial oscillator, injection locking is possible, but then the impedance is only known at the circulator terminals ($T_F^* - T_F$ in Fig. 6) where the injected signal is inserted. Since the equivalent

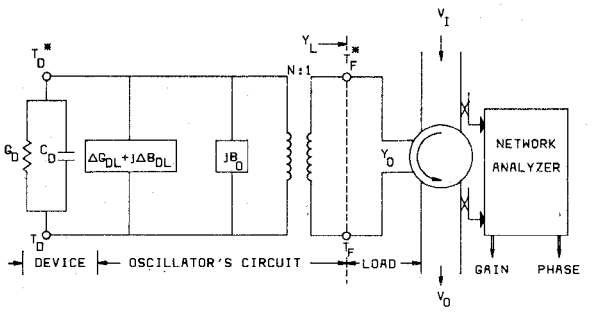

Fig. 9. The transformer representation of the equivalent circuit used for analysis of the injection-locked measurements of the Gunn device in the coaxial cavity.

circuit for a coaxial resonator (analogous to Fig. 6) has not been developed, some method for obtaining the injection-locked impedance at the device terminals $(T_D^*-T_D)$ is needed as given below.

When a transmission line A makes an arbitrary transition to a transmission line B of length L_B terminated by an arbitrary load impedance Z_L, a position L_A along A can be found so that the complex impedance at that point has the same phase angle as Z_L. If in addition, the transition is lossless, the incident energy is conserved by that dissipated in Z_L and that reflected back into A so that a simple transformer equivalent circuit can exactly model [13] the impedance transformation between L_A and Z_L. A special case occurs with a lossy transition if L_B is much less than a wavelength long. Then the transition loss can be included with Z_L, and the simple transformer impedance transformation can again be made. If this loss is known, a simple arithmetic correction transforms the real part of Z_L between its actual and adjusted values. The equivalent circuit for this transformer model of the Gunn device in the coaxial cavity as seen from the output power and signal injection terminal is shown in Fig. 9. The turns ratio N is determined [4] from the free-running case when $Y_L = Y_o$ at $T_F^*-T_F$ and from the impedance at the package terminals T^*-T which is directly measured (by reconnecting the network analyzer to this coaxial plane looking into the cavity without the packaged device) and then transformed by the package equivalent circuit to give the free-running admittance Y_{DL}^F at the device terminal plane $T_D^*-T_D$. This gives

$$N^2 = \frac{Y_o}{Y_{DL}^F}. \tag{A1}$$

Returning the Gunn device to the coaxial cavity then allows injection locking and variation of the load admittance Y_L as specified by (9). In this approach, the device negative conductance is then simply given as

$$G_D = \frac{-Y_o}{N^2}\left[\frac{1-\rho^2}{1+\rho^2+2\rho\cos\phi}\right] \tag{A2}$$

and the RF voltage by

$$V_{\mathrm{RF}} = N\left[\frac{2P_o}{Y_o}\right]^{1/2}\left[1+\rho^2+2\rho\cos\phi\right]^{1/2}. \tag{A3}$$

References

[1] Y. Ito, H. Komizo, T. Meguro, Y. Daido, and I. Umebu, "Experimental and computer simulation analysis of Gunn diode," *IEEE Trans. Microwave Theory Tech.*, vol. MTT-19, pp. 900–905, Dec. 1971.

[2] D. D. Khandelwal and W. R. Curtice, "A study of the single frequency quenched-domain mode Gunn-effect oscillator," *IEEE Trans. Microwave Theory Tech.*, vol. MTT-18, pp. 178–187, Apr., 1970.

[3] H. L. Hartnagel and M. Kawashima, "Negative TEO-diode conductance by transient measurement and computer simulation," *IEEE Trans. Microwave Theory Tech.*, vol. MTT-21, pp. 468–477, July 1973.

[4] J. C. T. Young and I. M. Stephenson, "Measurement of the large-signal characteristics of microwave solid state devices using an injection-locking technique," *IEEE Trans. Microwave Theory Tech.*, vol. MTT-22, pp. 1320–1323, Dec. 1974.

[5] W. M. Sharpless, "Wafer-type millimeter wave rectifiers," *Bell Syst. Tech. J.*, pp. 1385–1403, Nov. 1956.

[6] T. P. Lee and R. D. Standley, "Frequency modulation of a millimeter-wave IMPATT diode oscillator and related harmonic generation effects," *Bell Syst. Tech. J.*, vol. 48, pp. 143–161, 1969.

[7] J. Bybokas and B. Farrell, "The Gunn flange—A building block or low-cost microwave oscillators," *Electronics*, vol. 41, pp. 47–50, Mar. 1971.

[8] M. R. Lakshminarayana and L. D. Partain, "Numerical simulation and measurement of Gunn device microwave characteristics," *IEEE Trans. Electron Devices*, vol. ED-27, pp. 546–552, 1980.

[9] W. J. Getsinger, "The packaged and mounted diode as a microwave circuit," *IEEE Trans. Microwave Theory Tech.*, vol. MTT-14, pp. 58–69, Feb. 1966.

[10] W. J. Getsinger, "Mounted diode equivalent circuits," *IEEE Trans. Microwave Theory Tech.*, vol. MTT-15, pp. 650–651, Nov. 1967.

[11] R. P. Owens and D. Cawsey, "Microwave equivalent—Circuit parameters of Gunn-effect device packages," *IEEE Trans. Microwave Theory Tech.*, vol. MTT-18, pp. 790–798, Nov. 1970.

[12] J. Heaton and T. B. Ramachandran, "Measurement of Gunn diode thermal resistance," *Microwave J.*, vol. 19, pp. 43–46, Aug. 1976.

[13] N. Marcuvitz, *Waveguide Handbook*, (vol. 10, MIT Radiation Laboratory Series). New York: McGraw-Hill, 1951.

[14] K. Kurokawa, *An Introduction to the Theory of Microwave Circuits*. New York: Academic Press, 1969.

[15] K. Kurokawa, "Some basic characteristics of broadband negative resistance oscillator circuits," *Bell Syst. Tech. J.*, vol. 48, pp. 1937–1955, July–August, 1969.

[16] R. Alder, "A study of locking phenomena in oscillators," *Proc. IRE*, vol. 34, pp. 351–357, June, 1946.

[17] L. J. Paciorek, "Injection locking of oscillators," *Proc. IEEE*, vol. 53, pp. 1723–1727, Nov. 1965.

[18] M. Michaelides and Stephenson, "Injection locking of microwave solid state oscillators," *Proc. IEEE*, vol. 59, pp. 319–321, Feb. 1971.

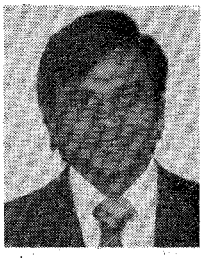

Mysore R. Lakshminarayana (S'75–M'77) was born in Sira, Karnataka, India. He received the B.E. degree from Bangalore University, India, in 1969, and the M.E.E. and Ph.D. degrees in electronic engineering from University of Delaware, in 1974 and 1978, respectively.

From 1969 to 1970 he was a Lecturer in Electronic Engineering at Mysore University, Mandya, India. From 1970 to 1977 he was a Research Fellow and Teaching Assistant at University of Delaware, where he did research on electronic transport properties of semiconductors, and microwave devices and systems. From 1977 to 1978 he worked as a Post Doctoral Research Fellow. He did research on microwave modulation of lasers and integrated optics. He is presently an Associate Professor in the Department of Electrical and Computer Engineering at California State Polytechnic University,

Pomona, California. His current research interests include microwave circuits, fiber optics, and laser applications.

Dr. Lakshminarayana is a member of Eta Kappa Nu.

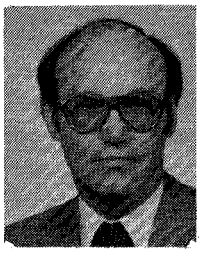

Larry D. Partain (S'64–M'72) was born in McKinney, Texas, in 1942. He received the B.S. degree in electrical engineering from the University of Tennessee in 1965 and the Ph.D. degree in electrical engineering from Johns Hopkins University in 1972.

He was appointed Assistant Professor of Electrical Engineering and Materials Science at the University of Delaware in 1971 and Associate Professor in 1976. In 1978 he joined the Engineering Research Division of the Lawrence Livermore Laboratory as a co-principal investigator in the Device and Effects Group of the Engineering Research Division. Since 1980 he has been with the Solar Division of the Chevron Research Company where he is the leader of the Device Physics Group. In addition to microwave devices, his research has dealt with low-cost thin-film solar cells and with Hall-effect devices.

Hold-In Characteristics of an Extended Range Gunn Oscillator System

B. N. BISWAS, S. K. RAY, K. PRAMANIK, M. SADHU AND D.BANDYOPADHYAY, STUDENT MEMBER, IEEE

Abstract — **This paper describes a new Gunn oscillator system having an additional arrangement for controlling the instantaneous frequency of the oscillator through an automatic frequency control circuit. By utilizing this new technique, based upon the principle of self tracking, the locking bandwidth of an injection-locked Gunn oscillator can be increased to a large extent without affecting its stability. Experimental observations are found to be in good agreement with the conclusions of the analytical approach.**

I. Introduction

IN THE LAST several years, quite a lot of work has been done on the various aspects of an injection-locked Gunn oscillator. As a result, it has been shown that an attempt to increase the locking bandwidth of an injection-locked Gunn oscillator by increasing the strength of the incoming signal is always accompanied by the manifestation of an asymmetric character of the locking bandwidth, i.e., the hold-in ranges on the two sides of the center frequency of the oscillator become different [1], [2]. Moreover, it is not always possible to increase the strength of the synchronizing signal. On the contrary, the strength of the synchronizing signal is usually low. Therefore, the purpose of this paper will be to develop an injection-synchronized Gunn oscillator system that will have a much wider bandwidth than that of an ordinary injection-locked Gunn oscillator, even if the strength of the incoming signal is low. It is also shown that in the proposed system the asymmetric nature of the locking characteristic can be reduced to a great extent. This will be demonstrated both theoretically and experimentally in the sections to follow.

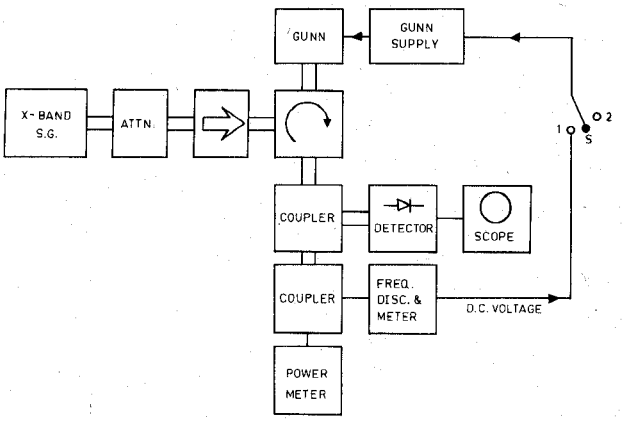

Fig. 1. Schematic representation of the proposed system.

II. Description of the System

The proposed Gunn oscillator system is shown in Fig. 1. It is basically a dual control system consisting of a Gunn oscillator, a frequency discriminator, and an arrangement for controlling the Gunn bias. The output of the Gunn oscillator is fed to the frequency discriminator, the output of which in turn controls the instantaneous frequency and amplitude of the Gunn oscillator through the variation of the bias voltage.

Manuscript received June 8, 1982; revised November 2, 1982. This work was supported in part by the Department of Science and Technology, Government of India.

The authors are with the Radionics Laboratory, Physics Department, Burdwan University, Burdwan 713 104, India.

0018-9480/83/0300-0271$01.00 ©1983 IEEE